

Power-Sharing of Parallel Inverters in Micro-Grids via Droop control and Virtual Impedance

Samia Abdalfatah¹, Mohammed Gamal², E.E. Elkholy³, Hilmy Awad⁴

¹Faculty of Technology and Education, Helwan University, Egypt,

²Electricity Teacher, Industrial Secondary School, Menoufia,

³Engineering Department, Faculty of Engineering, Menoufia University, Egypt,

⁴Faculty of Technology and Education, Helwan University, Egypt.

Abstract – The inverter based small networks connected in parallel, the inverters can operate in connected or separate network mode, and in the connected mode, the set points for each inverter are created by processing data on the active output powers and placing all the inverters in a principal controller based on the needed output power ratios. Here, two proposed power-sharing structures are used to provide a fast and accurate dynamic response to a low circulating current between parallel inverters and the ability to adapt to the required changes in the system to make it stable and make each inverter give its full capacity to the loads. In this article, two different types of system control are used to share energy through electrical inverters. The droop control and virtual impedance are used, and each system improves the performance of the control in a better way to share the load energy. The proposed energy-sharing control systems strategies have been validated using mat-lab/Simulink simulation results

Keywords: Droop Control; Micro-grid control; Power Sharing; parallel inverter; line impedance.

1. INTRODUCTION

The integration of several distributed energy resources (DERs) that are linked in parallel, such as parallel inverters in micro-grid operation, is necessary to meet the growing need for large-scale power supply with high dependability [1]. Advanced control techniques are necessary for parallel inverters to operate properly. Many of these methods were first presented decades ago, and they are still developing today [2]. a frequency-voltage droop approach is a well-recognized widely used, and successful method for operating parallel inverters [3]. this method simulates how a large-scale power system works by using a pre-set droop feature that links improvements in generator speed and output active power. This technology is known as wireless control since no communication is necessary between the inverters making it simple to deploy and dependable [4]. But, it has various drawbacks that might hinder its effectiveness. Some of its limitations were just as described in the following: its frequency and amplitude differences are load dependent, resulting in poor load voltage regulation performance; an inherent trade-off between voltage regulation and power

sharing between inverters, and impedance mismatch among inverters affects power sharing performance [5].

Many improvements have been proposed in recent years to increase the effectiveness of the droop control approach in order to satisfy the rising needs of micro-grids. Modified droop [6-8], adaptive droop [9-11], mixed droop [12-14], and interconnected droop working principle [15-18] are some of the suggested changes. A standard droop system is given a boost in transient responsiveness in [6] by the addition of power derivative-integral terms. Selecting the proper coefficients for the derivative term, however, in order to guarantee stable system performance, is challenging. The authors of [11] suggested combining static droop features with an adaptive transient droop function to enable active dampening of power oscillations. The authors did not, however, provide experimental confirmation for this method. The authors of [16] presented an enhanced droop method that employs web-based limited bandwidth connection to enhance load-sharing ability. This performance realizes efficient electric power-sharing with the micro grid. A droop control with an optimization system is presented in [13]. It uses particle cloud optimization to optimize the (v-f) constant. It shows respectable active and reactive power sharing in simulation, but there is no hardware confirmation.

Inverters linked in parallel have lately come to understand that exchanging certain information among them may help accomplish great current sharing and voltage management in a parallel system. Active load-sharing methods are a few examples of control strategies that make use of communication between parallel inverters. These include the average current configuration [21, 22], the master-slave system [19, 20], and the spherical current technique.

In the circular-chain current approach, succeeding inverter modules follow the current of the preceding inverter to achieve equal current circulating. The fundamental flaw with this strategy is that it significantly relies on communications, which introduces substantial uncertainties into the system. The master/slave approach employs one inverter to control the amplitude and frequency, while the remaining inverters serve as slaves that inject currents. All of the micro grid's inverters participate in the typical current-sharing mechanism, which regulates voltage, frequency, and current.

In particular, the inverter current injection averaged over a common bus is taken into account as a reference for each module when determining the average current data.

Active load sharing approach has unique benefits and drawbacks. There are many different ways to solve the problem, from communication to techniques that need less communication. To avoid overheating and maintain a longer lifespan, some applications have strict loading requirements for the inverters, and correct active and reactive power sharing is essential. These implementations will be made easier by having the ability to change the power references while maintaining precise sharing and damped responsiveness. Therefore, a control scheme that is adaptable, trustworthy, and has strong voltage stability, current sharing, and decreased current flowing features is preferred. It should also have minimal reduced communications and be resistant to communication overhead.

In this article, a comparison will be made between two different power-sharing technologies. In this paper, a comparison will be made between two other power-sharing techniques (droop controller and virtual impedance), which uses fuzzy logic, and necessarily requires a low-bandwidth connection to a central controller. All of the parallel inverters that are connected to the central control unit send information about their active and reactive power, and it uses that data to calculate each inverter's active and reactive power references. Based on a particular ratio of output power to each inverter, these references are computed. This information is used by each inverter to modify the voltage and amplitude reference phase in relation to the shared AC vector in order to achieve the required output power. By adjusting the phase rather than the frequency, as a result, it is possible to achieve effective frequency regulation without affecting the nature of the various filters LCL and LC used to share power between inverters connected in parallel with the grid between power and load sources for system stability. The overall design of the inverter is shown in figure 1. The voltage controller transmits modulated sine waves to its IGBT switching components, which begin receiving them. The system contains two solar cell networks, in which the maximum power is obtained through Perturb and Observe (o & p) [33]. The two networks are connected from the side of the inverter output. The inverter is controlled through the two techniques. Below is a simplified explanation of each part of the system.

five sections make up the structure of this term paper Section (2 and 3) discusses the system architecture One of the fundamental problems of parallel inverters is the robust design of each inverter operating in parallel with the power grid and the proposed power -sharing method, as A stability study of the proposed technologies for virtual impedance and system control algorithm, which has a maximum power point tracking MPPT photoelectric controller, is presented in

Section (4). Analysed in a mat-lab environment Simulink simulation results in variable weather conditions are shown in Sections (5) to support the feasibility and efficacy of the proposed method respectively, the conclusions emphasize the main results and the ability to contribute to this article.

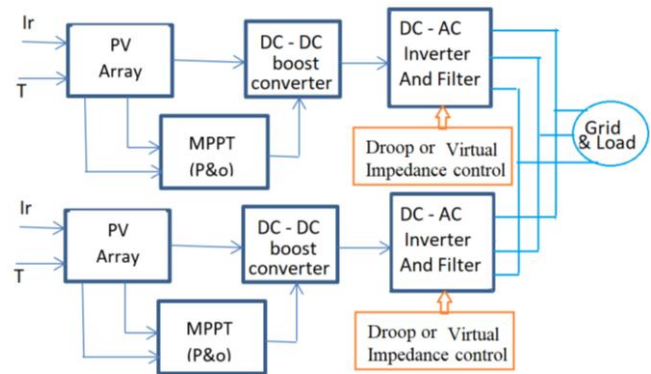


Fig-1: General micro grid Structure

1.1 Photo voltaic (P.V) System

A PV module consists of several solar cells connected in series and parallel to obtain the desired voltage & current output levels shown in Fig 2. PV consists of a photocurrent source I_{ph} , diode, and internal resistances R_S and R_p [35, 36].

I_{ph} : Light produced current (A).

I_D : Diode saturation current (A).

I_o : reverse saturation current of the diode

q : electron charge ($1.6 \times 10^{-19} C$)

K : Boltzmann constant in $1.3865 \times 10^{-23} (J/K)$

μ : conversion efficiency (%)

I_a : current through the diode

T_c : operating temperature ($^{\circ}C$)

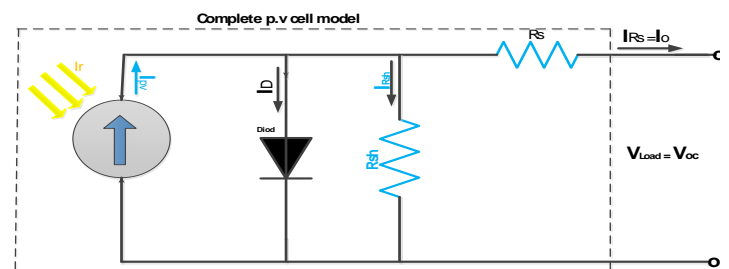


Fig-2: Model for a solar cell

Parasite resistivity is a component of a functional photovoltaic array.

Due to the continued resistance of the interconnections metal grid, p and n layer, there is series resistance

Shunt resistivity brought on by p-n connection leakage current.

A PV system is physically described in the following equations [35, 36].

$$I_{pv} = N_p \cdot I_{ph} - N_p \cdot I_d - I_{sh} \tag{1}$$

$$I_{ph} = [I_{sh} + K_i (T_c - T_{ref})] \left(\frac{I_r}{1000} \right) \tag{2}$$

$$I_d = I_s \left[e^{\frac{q \cdot V_d}{\alpha K T N_s N_p}} \right] - 1 \tag{3}$$

$$I_s = I_{rs} \left(\frac{T_c}{T_{ref}} \right)^3 \left[e^{\frac{q \cdot E_g}{K \cdot \alpha} \left(\frac{1}{T_{ref}} - \frac{1}{T_c} \right)} \right] \tag{4}$$

The solar module's efficiency is determined by dividing the greatest amounts of electricity it can generate by solar irradiation [28].

$$\mu = \frac{P_{MPP}}{P_{in}} = \frac{V_{MP} I_{MP}}{P_{sun}} \tag{5}$$

1.2 Maximum Power Point Tracking (MPPT)

Tracking the PV array's greatest peak power in order to produce the most electrical power is the crucial step for photovoltaic arrays. The best procedure should be followed during the design of the PV system, and various MPPT methods can be used to ensure this [23]. It depends on irradiance and temperature. There are various layers in each strategy. Application characteristics, including those of the most iconic one, the hill climbing technique on the resilience of two points, can have a significant impact on the choice of MPPT control systems, including complexity sensors, amount of digital or analogue applications, rapid convergence traceability, and financial impact. P(k), p (k-1) Start comparing MPPT and MPP side by side.

The primary benefit of strategic is that it is inexpensive, simple to implement, does not require a control scheme or micro - controller, and only requires one voltage sensor [17]. As long as the radiation from the sun does not fluctuate too much throughout the day, this method works well [28].

As shown in Fig.3 the suggested MPPT algorithm is perturbative and controls the dc - dc converter using feedback. A boost converter It increases the voltage value at the expense of the current value and deals with the constant current only and makes a comparison process between the voltage of a solar cell V_{pv} and the voltage inside the inverter V_{ref} .

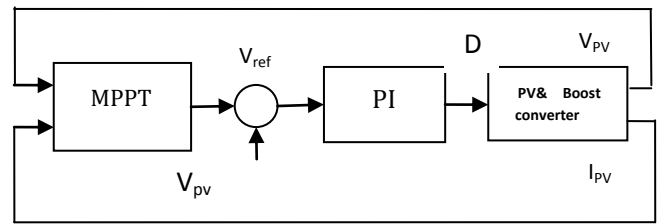


Fig-3: Schematic diagram of boost converter control.

In Fig.4 the photo - voltaic output power is plotted against the plate voltage for specific radiation. Traditional P&O technology [27,30] uses photovoltaic panels or current disruptions to continue operating and compares the power rating of the photovoltaic cell to the prior perturbation cycle. Features 1- Initial Restorative Dynamics

2- Analog /digital implementation

3- Minimal software/hardware requirements. The operating voltage in between the PV array and the converter is perturbed by the P&o method.

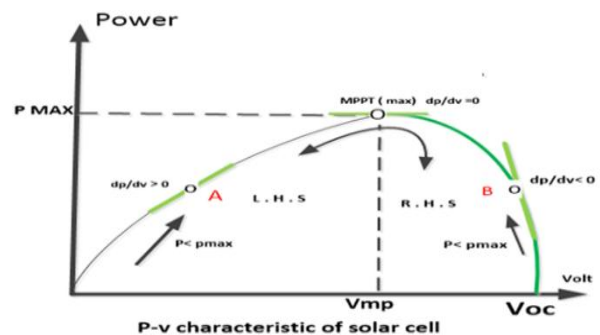


Fig -4: P&O Basic Idea Algorithm

P&O It consists of two main parts, Point A: $dP/dV > 0$ If the operating point on the left MPP and Point B: $dP/dV < 0$ If the operating point on the right MPP, $dP/dV = 0$ At the operating point on the MPP Turbulent is employed in voltage and power measurement methods, and the high value utilization of the turmoil direction is calculated by

$P\Delta = (P2 - P1)$. If the polarization of a power output is positive, a next disturbance will travel in same directions as the prior one. If the depolarization of a power output is negative, a next disturbance is in the reverse direction as the prior one. When MPP is attained, the operation is repeated.

1.3 DC/AC Inverter and LCL Filter

the inverter as shown in the image(5) converts dc to ac current and must be included in any micro-network that uses electrical power electronics to serve single or three-phase loads consisting of high frequency solid-state electronics and an L - LCL low-pass filter it is in charge of smoothing the output wave in order to achieve a sinusoidal signal free of harmonics the inverter has a steady current

input and is linked to a capacitor which stabilizes and regulates the voltage energy from solar cells and raises it to the inverter the output is the ac current produced at the inverters output signals are sent by the voltage controller to the switching devices which are isolated gated bipolar transistors (IGBT) V_{ref} and P.W.M signals are generated in addition when the A.C signal of the power electronic switches changes harmonic signals are created the LCL filter is widely used in conjunction with inverse networks to enhance current excellence and supply optimum sinusoidal power to a power grid while minimizing harmonics.

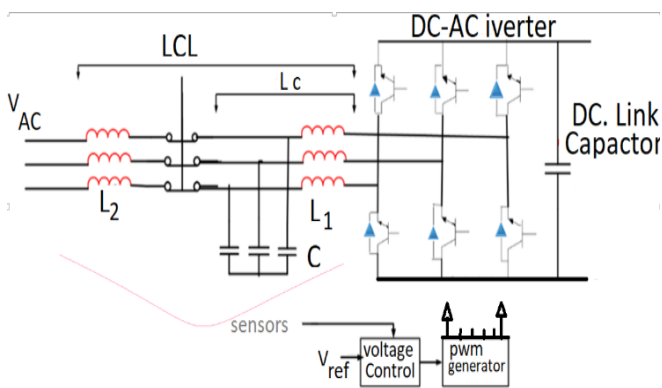


Fig -5: inverter and LCL filter

2. Virtual impedance technology

A voltage controller loop is used in basic voltage source inverters VSI to track the desired input signal and reduce its error and the measured output voltage. A proportional controller, K_v , is utilized in this study, backed by a feed-forward loop. The feed-forward loop reduces steady-state error while allowing for a broader control band [1,3].

Fig.5 depicts one inverter phase. Their inner loop controllers are shown in this block diagram [12,14]. In this paper, ("Virtual Impedance Impact on Inverter Control Topologies") This impedance mimics the behavior of an inductor or resistor in the program. Using a programmable impedance rather than a physical one reduces the losses and costs [19,22]. In addition, being programmable presents adaptive operation and increases the inverter's robustness against network impedance variations [23,27]. Fig. 6 shows the block diagram of the voltage controller with the virtual impedance $Z_v(s)$.

$$V_o(s) = G(s) * V^*(s) - Z_{ov}(s) * I_o(s) \tag{6}$$

The output impedance with virtual impedance can be derived as, ("Virtual Impedance Impact on Inverter Control Topologies")

$$Z_{ov}(s) = Z_o(s) + G(s) Z_v(s) \tag{7}$$

The nature of Z_v could be chosen to be resistive as,

$$Z_v(s) = R_v \tag{8}$$

Where R_v is the resistance of the virtual impedance, or it can be inductive as

$$z_v(s) = \frac{s}{\tau_v s + 1} L_v \tag{9}$$

Where L_v is the inductance of the virtual impedance and is τ_v the time constant of the high pass filter used to approximate the derivative in the transfer function of the ideal virtual inductance $Z_v = sL_v$ [25].

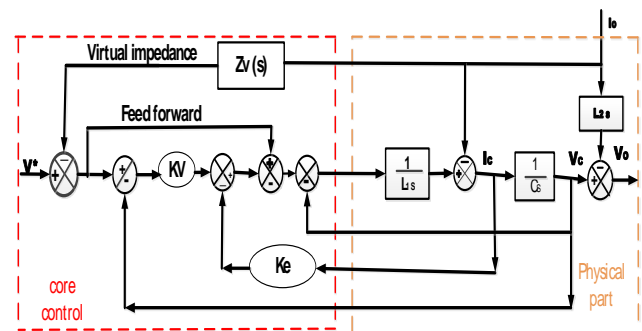


Fig -6: The model of basic double-loop voltage controller

3. Droop control technology

In this paper, a micro-grid consisting of two inverters as shown in Fig.1 is considered. The circuit diagram of each inverter and its LCL filter and controller is illustrated in Fig. 7. This is the basis for the conventional droop characteristic, as represented in (8) and (9) [6].

$$V = V^* - n(Q - Q^*) \tag{10}$$

$$\omega = \omega^* - m(P - p^*) \tag{11}$$

Where ω^* , V^* are the nominal frequency and nominal voltage references, m and n are the frequency- proportional drooping coefficient and voltage-proportional drooping coefficient, respectively. The droop slopes are determined according to the power rating of the inverter and according to the maximum allowable variations in output frequency and voltage [11,13]. In grid-connected mode, the active and reactive power set-points p^* and Q^* are adjusted to be equal to the reference power values. The conventional droop characteristic is summarized in Fig.8. In this figure, the loaded active- and reactive power is denoted along the x-axes. As shown, an increased active load leads to a reduction in the frequency, while the output voltage is reduced if a more reactive load is added to the system. This characteristic can be utilized in the conventional droop control method, where the active power fed into the line is controlled based on frequency deviations, while deviations in voltage control the reactive power supply. The deviations are determined by

the droop coefficients, which are given based on (10) and (11) [36,26].

$$m = \frac{\Delta \omega_{max}}{P_{change}} \tag{12}$$

$$n = \frac{\Delta V_{max}}{Q_{change}} \tag{13}$$

$\Delta\omega_{max}$ is the maximum allowed frequency deviation due to a load change in active power, P_{change} . The maximum allowed voltage change, ΔV_{max} , is in a similar way related to a load change in reactive power, Q_{change} . Often, $\Delta\omega_{max}$ and ΔV_{max} are decided based on the maximum deviations allowed in the grid. The droop coefficients also affect the power sharing among inverters, where larger droop coefficients lead to better power sharing. However, the coefficients have upper limits, where increasing them would lead to instability in the system. Within the stability limits,

the choice of droop coefficients is a trade-off between the power sharing performance and the deviations in voltage and frequency. [15,17].

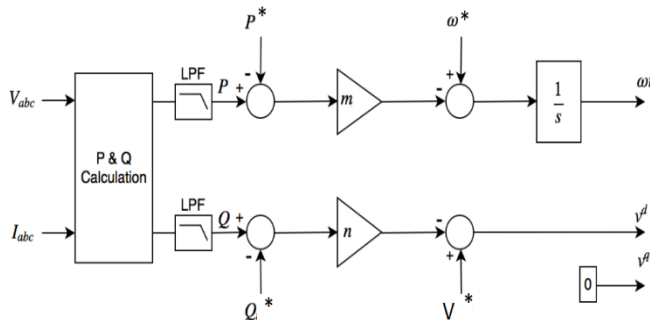


Fig -7: Implementation of the conventional droop control

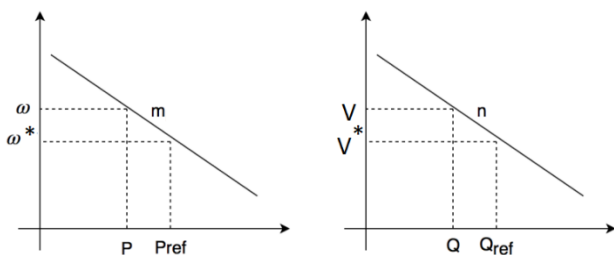


Fig -8: The characteristic of the conventional droop control

4. SIMULATION RESULTS AND DISCUSSION

This section illustrated the performance of PV module and performance of perturb and observe algorithm to track maximum power point of PV module under various weather conditions. The PV module simulation is implemented in MATLAB Simulink. The parameter of the PV module (330 Sun Power modules). is displayed for one module is:

Number of parallel-connected cells: 39 cell

Number of series-connected cells: 5 cell

shows Fig.9 shows the power-voltage characteristic of PV module in four cases, and Fig.10 shows the sun's radiation of value.

To verify the performance of the simulation that was conducted on MATLAB / Simulink, to compare two different technologies, namely, the virtual impedance and the traditional droop control to control the electric power output to share the electric loads with the main network. The micro-grid contains two electrically identical stations conditioned by variable solar radiation ranging between 250 and 1000 W/m² at a constant temperature of 25 °C.

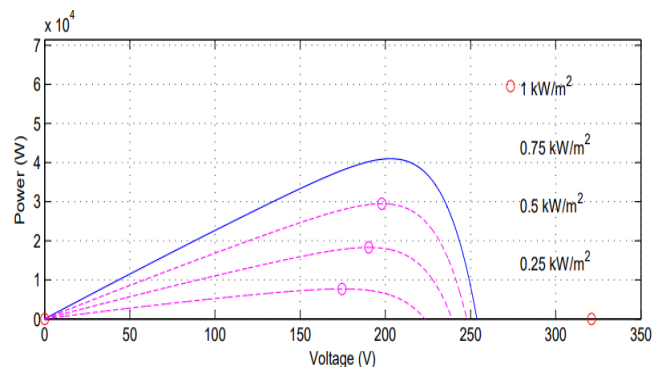


Fig-9: Characterizes of photovoltaic

The efficiency of the P.V system in various weather conditions and turbulence is also as a monitoring method used to track the highest energy point. The photovoltaic module characteristic shows the (60) kW photovoltaic cell in the proposed model consisting of (330) solar modules. The PV module parameters for a single module are shown as follows:

It is clear from Fig .10 that the number of panels connected in series (5) successive stages

- T= (0-0.5) sec: with a radiation intensity of (200) W/ m² at a constant temperature (25 °C), then the intensity of solar radiation increases to 1000 W/m² gradually
- T= (0.5-2) sec: the radiation intensity remains constant,
- T= (2-4) sec: the radiation intensity gradually decreases until it reaches (300) W/m²
- T= (4-5) sec: the radiation intensity gradually decreases from 300 to zero.
- T= (5-6) sec: the radiation intensity becomes (0), meaning that the two stations exit the system and give electrical energy = 0, and the load derives its energy from the electrical grid.

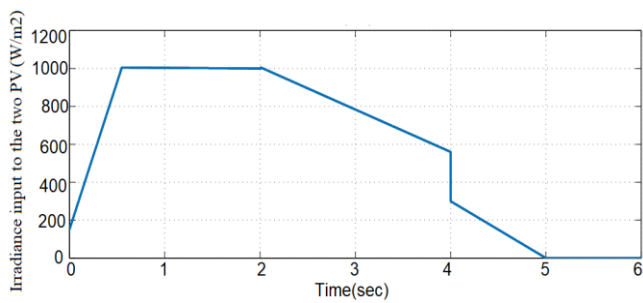


Fig -10: Irradiance input to the PV array

The active power output curve of the photovoltaic cells over time with a variable solar irradiance value from 200 to 1000 W/m^2 as in Figure11 and at a constant 25°C. The maximum value of the capacity of the solar cells is 60 kW, and with the change of solar radiation over time, when the system starts in the first 0.5 sec, a sudden change in the value of electric energy occurred when using the virtual impedance technology to share the electric power of the loads with the micro grid.

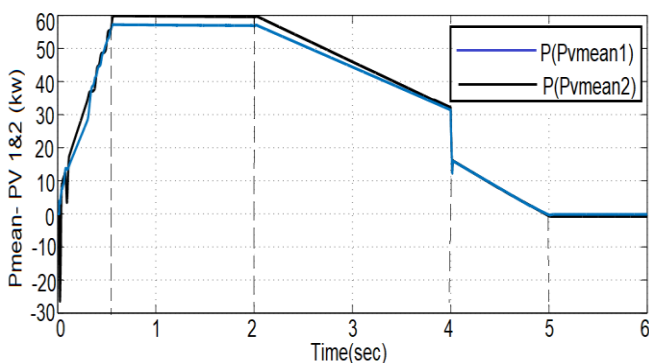


Fig -11: Active power mean of the two PV

Case study (1): Simulation results if no droop control technique or no virtual impedance is applied to share the output power of two identical micro-grid inverters.

Figure 12 illustrates the output power of each inverter. It is assumed that both inverters are already operating in parallel and that the without power sharing. We note that the output of the second reflector (P_{pv2}) gives its full value, while the first (P_{pv1}) reflector gives a much lower value with the change in solar radiation. the power responses lost the stability.

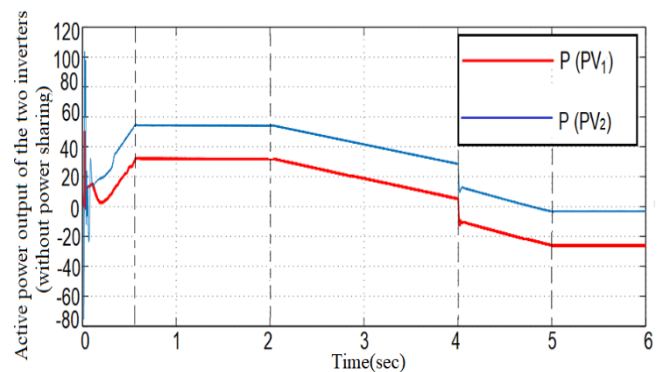


Fig-12: Active power output of the two inverters
(without power sharing)

Case study (2): Simulation results when using the virtual impedance control technique to share the active power of two Identical inverters connected to the micro-grid have the same output power.

Fig.13 shows the output power of each inverter. It is assumed that both inverters work together in parallel as the inverter is controlled by controlling the voltage source using the virtual impedance. Where it was found from the operation that the output capacity of the first inverter (which output is connected to a filter of type LCL) does not reach its maximum power, but is lowered from it by a simple value

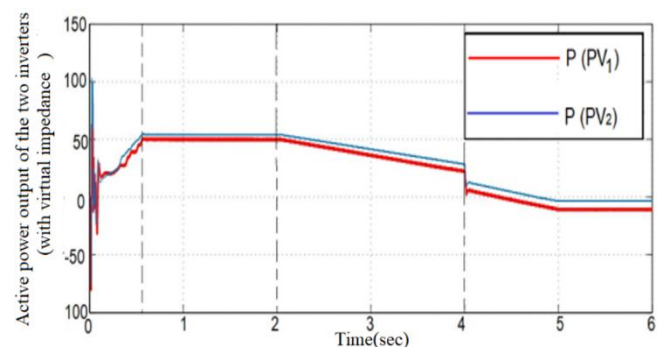


Fig-13: Active power output of the two inverters
(with virtual impedance)

Case study (3): Simulation results when using the droop control technique to share the output power of two Identical inverters connected to the micro-grid.

Fig.14 shows the output power of each inverter. It is assumed that both inverters work together in parallel as the inverter is controlled by voltage source control using droop control. The process shows that the output capacitance of the first inverter (which output is connected to a LCL-type filter) has a fast response and achieves cooperation with the change in the value of the output power of the solar cells.

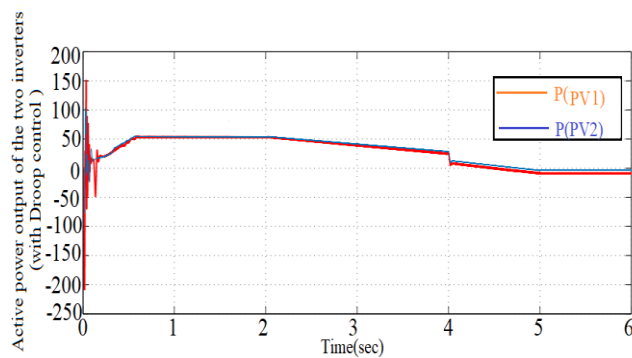


Fig -14: Active power output of the two inverters (with droop control)

5. Conclusion

In this article, two methods of output power sharing between inverters connected in parallel with the micro-grid, namely droop control and virtual impedance, are proposed to be applied to AC networks to ensure high accuracy and flexibility in electric power sharing. And we conclude from the results obtained from simulations in the Mat-lab / Simulink environment for two parallel inverters can be painted:

- When virtual impedance control is applied in a small grid system as a technique for sharing electrical energy between inverters with fuzzy used to improve the output shape of the effective power, it does not work well under these changing conditions, as the effective power sharing is affected by the virtual impedances in the small grid between the inverters. Transformers and PCC during the sharing process.
- To overcome this problem, the proposed droop control technique is applied to adjust the line resistance value to properly share the effective power between the inverters and work better under the same conditions even when there are differences in the line resistance in a small network.
- The voltage droop can be reduced in the proposed droop control technique.
- Swing control The ability to quickly switch according to the proportions of the active electrical power accurately.

When implementing a proposed micro-grid with VSI transformers parallel to the electrical network for supplying connected electrical loads, consideration should be given to: DC sources with galvanic isolation; Determines the total electrical capacity of the load. In addition, the controller controls each of the VSI switches connected to the micro-network so that no interference occurs and the system is balanced, stable, and works well.

It has been scientifically proven from the simulation results that the proposed droop control method is superior and works better and more accurately while making the system

balanced and stable ineffective force sharing when the line resistance is actually changed from the default impedance technology, plus it does not need human intervention.

Table -1: Comparison between Droop control and Virtual impedance

Comparison scheme	(v/f)Droop control technique	Virtual impedance scheme
Capability to set power ratio	Yes, without the need for fuzzy	Yes, but needs a fuzzy
Advantage	<ul style="list-style-type: none"> - Fast dynamic response at the start of the operation - Very flexible and has the ability to expand. -System stability and power sharing accuracy -It is not affected by any fundamental change in the system -Ease of implementation in the absence of contact between the inverters 	<ul style="list-style-type: none"> -Can be used with linear and non-linear loads when electric power is shared - Reduces harmonic voltage -Decoupled active and reactive power controls
Dis advantage	<ul style="list-style-type: none"> -Inaccurate voltage and frequency regulation 	<ul style="list-style-type: none"> -Low dynamic response -It is necessary to know the physical variables first -Inaccurate voltage and frequency regulation -Affected by any physical change in the system - The system is unstable, especially when starting, and less accurate in sharing electric power

REFERENCES

- [1] W. R. Issa, A. H. E. Khateb, M. A. Abusara, and T. K. Mallick, "Control strategy for uninterrupted microgrid mode transfer during unintentional islanding scenarios," *IEEE Transactions on Industrial Electronics*, vol. 65, no. 6, pp. 4831–4839, 2018. View at: [Publisher Site](#) | [Google Scholar](#)
- [2] P. Sreekumar and V. Khadkikar, "Adaptive power management strategy for effective volt-ampere utilization of a photovoltaic generation unit in standalone microgrids," *IEEE Transactions on Industry Applications*, vol. 54, no. 2, pp. 1784–1792, 2018. View at: [Publisher Site](#) | [Google Scholar](#)
- [3] W. R. Issa, M. A. Abusara, and S. M. Sharkh, "Control of transient power during unintentional islanding of microgrids," *IEEE Transactions on Power Electronics*, vol. 30, no. 8, pp. 4573–4584, 2015. View at: [Publisher Site](#) | [Google Scholar](#)
- [4] *Transactions on Power Electronics*, vol. 30, no. 8, pp. 4573–4584, 2015. View at: [Publisher Site](#) | [Google Scholar](#)
- [5] M. Hossain, H. Pota, W. Issa, and M. Hossain, "Overview of AC microgrid controls with inverter-interfaced generations," *Energies*, vol. 10, no. 9, p. 1300, 2017. View at: [Publisher Site](#) | [Google Scholar](#)
- [6] W. Issa, S. Sharkh, T. Mallick, and M. Abusara, "Improved reactive power sharing for parallel-operated inverters in islanded microgrids," *Journal of Power Electronics*, vol. 16, no. 3, pp. 1152–1162, 2016. View at: [Publisher Site](#) | [Google Scholar](#)
- [7] J. M. Guerrero, L. Garcia de Vicuna, J. Matas, M. Castilla, and J. Miret, "A wireless controller to enhance dynamic performance of parallel inverters in distributed generation systems," *IEEE Transactions on Power Electronics*, vol. 19, no. 5, pp. 1205–1213, 2004. View at: [Publisher Site](#) | [Google Scholar](#)
- [8] W. R. Issa, M. A. Abusara, and S. M. Sharkh, "Impedance interaction between islanded parallel voltage source inverters and the distribution network," in *IET Conference Publications*, 2014, vol. 2014, no.
- [9] S.-J. Ahn, J.-W. Park, I.-Y. Chung, S.-I. Moon, S.-H. Kang, and S.-R. Nam, "Power-sharing method of multiple distributed generators considering control modes and configurations of a microgrid," *IEEE Transactions on Power Delivery*, vol. 25, no. 3, pp. 2007–2016, 2010. View at: [Publisher Site](#) | [Google Scholar](#)
- [10] Y. W. Li and C. N. Kao, "An accurate power control strategy for power-electronics-interfaced distributed generation units operating in a low-voltage multibus microgrid," *IEEE Transactions on Power Electronics*, vol. 24, no. 12, pp. 2977–2988, 2009. View at: [Publisher Site](#) | [Google Scholar](#)
- [11] M. Wegmuller, J. P. von der Weid, P. Oberson, and N. Gisin, "High resolution fiber distributed measurements with coherent OFDR," in *Proc. ECOC'00*, 2000, paper 11.3.4, p. 109.
- [12] Y. Mohamed and E. F. El-Saadany, "Adaptive decentralized droop controller to preserve power sharing stability of paralleled inverters in distributed generation microgrids," *IEEE Transactions on Power Electronics*, vol. 23, pp. 2806–2816, 2008. View at: [Google Scholar](#)
- [13] M. N. Marwali, J.-W. Jung, and A. Keyhani, "Control of distributed generation systems-part II: load sharing control," *IEEE Transactions on Power Electronics*, vol. 19, no. 6, pp. 1551–1561, 2004. View at: [Publisher Site](#) | [Google Scholar](#)
- [14] I.-Y. Chung, W. Liu, D. A. Cartes, E. G. Collins, and S.-I. Moon, "Control methods of inverter-interfaced distributed generators in a microgrid system," *IEEE Transactions on Industry Applications*, vol. 46, no. 3, pp. 1078–1088, 2010. View at: [Publisher Site](#) | [Google Scholar](#)
- [15] S. T. Cady, A. D. Dominguez-Garcia, and C. N. Hadjicostis, "A distributed generation control architecture for islanded ac microgrids," *IEEE Transactions on Control Systems Technology*, vol. 23, no. 5, pp. 1717–1735, 2015. View at: [Publisher Site](#) | [Google Scholar](#)
- [16] Y. Zhang and H. Ma, "Theoretical and experimental investigation of networked control for parallel operation of inverters," *IEEE Transactions on Industrial Electronics*, vol. 59, no. 4, pp. 1961–1970, 2012. View at: [Publisher Site](#) | [Google Scholar](#)
- [17] R. Majumder, G. Ledwich, A. Ghosh, S. Chakrabarti, and F. Zare, "Droop control of converter-interfaced microsources in rural distributed generation," *IEEE Transactions on Power Delivery*, vol. 25, pp. 2768–2778, 2010. View at: [Google Scholar](#)
- [18] Ch, Sai Babu & Kumari, J. & Kullayappa, T. (2011). "Design and Analysis of Open Circuit Voltage Based Maximum Power Point Tracking for Photovoltaic System". *International Journal of Advances in Science and Technology*. 2. 51-60. tronics, 55, 2610-2621.
- [19] R. Issa, T. K. Mallick, and M. Abusara, "Supervisory control for power management of an islanded AC microgrid using a frequency signalling-based fuzzy logic controller," *IEEE Transactions on Sustainable Energy*,

- vol. 10, no. 1, pp. 94–104, 2019. View at: Publisher Site | Google Scholar
- [20] T. F. Wu, Y. K. Chen, Y. H. Huang, W. Tsai-Fu, C. Yu-Kai, and H. Yong-Heh, "3C strategy for inverters in parallel operation achieving an equal current distribution," *IEEE Transactions on Industrial Electronics*, vol. 47, no. 2, pp. 273–281, 2000. View at: Publisher Site | Google Scholar
- [21] Y. Pei, G. Jiang, X. Yang, and Z. Wang, "Auto-master-slave control technique of parallel inverters in distributed AC power systems and UPS," in *Proceedings of the 2004 IEEE 35th Annual Power Electronics Specialists Conference (IEEE Cat. No.04CH37551)*, Aachen, Germany, June 2004. View at: Publisher Site | Google Scholar
- [22] A. M. Roslan, K. H. Ahmed, S. J. Finney, and B. W. Williams, "Improved instantaneous average current-sharing control scheme for parallel-connected inverter considering line impedance impact in microgrid networks," *IEEE Transactions on Power Electronics*, vol. 26, pp. 702–716, 2011. View at: Google Scholar
- [23] Y. Xing, L. Huang, S. Sun, and Y. Yan, "Novel control for redundant parallel UPSs with instantaneous current sharing," in *Proceedings of the Power Conversion Conference-Osaka 2002 (Cat. No.02TH8579)*, Osaka, Japan, April 2002. View at: Publisher Site | Google Scholar
- [24] J. Femia, N. Lisi, G. Petrone, G. Spagnuolo, G. and Vitelli, M. (2008) *Distributed Maximum Power Point Tracking of Photovoltaic Arrays: Novel Approach and System Analysis*. *IEEE Transactions on Industrial Elec*
- [25] S.-H. Hu, C.-Y. Kuo, and T.-L. Lee, "Design of virtual inductance for droop-controlled inverter with seamless transition between islanded and grid-connected operations," *2012 IEEE Energy Conversion Congress and Exposition (ECCE)*, vol. 2012, pp. 4383–4387, 2012. View at: Publisher Site | Google Scholar
- [26] J. Padhye, V. Firoiu, and D. Towsley, "A stochastic model of TCP Reno congestion avoidance and control," *Univ. of Massachusetts, Amherst, MA, CMPSCI Tech. Rep. 99-02*, 1999
- [27] Omid Abdoli, Mehdi Gholipour Rahmatallah, Hooshmand "Improving synchronization stability of grid connected converters by virtual impedance" *IET Gener. Transm. Distrib.* 2021;15:1136–1143
- [28] T. Esum, P.L. Chapman, "Comparison of Photovoltaic Array Maximum Power Point Tracking Techniques," *IEEE Transactions on Energy Conversion*, vol. 22, no. 2, pp. 439–449, June 2007.
- [29] J. Aparna KP, Priya R, and S. Suryanarayanan, "Modeling and simulation of a PV system using DC-DC converter," *International Journal of Latest Research in Engineering and Technology (IJLRET)*, PP.09-16, vol. 1, no. 2, July, 2015
- [30] W. Issa, M. Abusara, S. Sharkh, and T. Mallick, "A small signal model of an inverter-based microgrid including DC link voltages," in *Proceedings of the 2015 17th European Conference on Power Electronics and Applications (EPE'15 ECCE-Europe)*, Geneva, Switzerland, September 2015. View at: Publisher Site | Google Scholar
- [31] W. Issa, A. El Khateb, N. Anani, and M. Abusara, "Smooth mode transfer in AC microgrids during unintentional islanding," *Energy Procedia*, vol. 134, pp. 12–20, 2017. View at: Publisher Site | Google Scholar
- [32] Abdelwahab, Saad & Hamada, Abdallah & Abdellatif, Walid. (2020), "Comparative Analysis of the Modified Perturb & Observe with Different MPPT Techniques for PV Grid Connected Systems", *International Journal of Renewable Energy Research*. 10. 155-164.
- [33] 32.M. Abusara, J. M. Guerrero, and S. Sharkh, "Line Interactive UPS for Microgrids," *IEEE Transactions on Industrial Electronics*, pp. 1-8, Mar 2014.
- [34] H. Tao, J. L. Duarte, and M. A. Hendrix, "Line-interactive UPS using a fuel cell as the primary source," *IEEE Transactions on Industrial Electronics*, vol. 55, pp. 3012–3021, Jul 2008.
- [35] K. Ashok Reddy, Kota Srinivas and G.S. Ayyappan "Power Management in a Standalone Solar/ Fuel cell/ Battery hybrid power systems" *International Journal of Engineering Research and Development*, Volume 9, Issue 6 December 2013 .
- [36] Erkan Dursun, Osman Kilie "Comparative evaluation of different power management strategies of a stand-alone PV/Wind/PEMFC hybrid power system" *international journal of Electrical power and energy systems*. Volume 34, Januar